Acoust. Sci. & Tech. **24**, 4 (2003)

PAPER

Acoustic source localization using phase difference spectrum images

Ryuichi Shimoyama* and Ken Yamazaki

Department of Electrical and Electronic Engineering, College of Industrial Technology, Nihon University, 1–2–1, Izumi-cho, Narashino, 275–8575 Japan

(*Received 22 May 2002, Accepted for publication 6 February 2003*)

Abstract: The localization of a single acoustic source on the horizontal plane using phase difference spectrum images is discussed. The azimuth for source is identified from the general linear relationship, which is extracted from the measured phase difference spectrum after filtering. The phase difference spectrum is introduced as the quasi-stationary cross-spectral phase between the sound signals detected simultaneously by two sensors. Acoustic source localization in an anechoic chamber having a metal base plate using two types of sound signals, white noise and voice, indicated that the phase difference spectrum was not affected with respect to the sound pressure level but was affected with respect to the azimuth for source. Although the phase difference spectrum measured in a reverberant room had less continuity as a function of frequency, a linear distribution of the images obtained from the data (dots) was observed on the frequency - phase difference plane. Using the phase difference spectrum images, the azimuths for various sources, which radiated any kind of broadband sound on separated time schedule, were precisely identified even in the reverberant room.

Keywords: Acoustic source localization, Images, Phase difference spectrum, Reverberant room

PACS number: 43.60.Pt, 43.66.Qp [DOI: 10.1250/ast.24.161]

1. INTRODUCTION

An algorithm to precisely identified various azimuths for source using only two sensors, as is the case with human the binaural system, is of great interest in several applications, such as acoustic source detection in humanoid robots, hearing aids, and acoustic security systems. Such an algorithm, by providing an analog to various human binaural functions, will also further our understanding of human information processing.

Several studies have examined the binaural model for human localization of an acoustic source [1–6], and approaches to the localization of an acoustic source via two sensors can be categorized into three primary types of algorithm and combinations thereof.

The first is the time delay (TD) between the sound pressure waveforms as detected by two sensors, which corresponds geometrically to the azimuth for source after being transformed to the propagation path difference [1,2,7–9]. Time delay, which gives the maximum correlation between two waveforms in time, is calculated numerically. Reverberation occasionally decreases the accuracy of time delay detection. The onset of the waveform is evaluated in detecting the time delay because the onset of the waveform is not influenced by reverberation. Environmental silence is required in order to estimate the azimuth for source in TD estimation.

Second, the level difference (LD) between two detected sound pressures, which is caused by the path difference, depends on the azimuth for source [1,2,10,11]. As LD is very susceptible to reverberation, the level difference spectral patterns for various source azimuths are recorded in advance and the arbitrary azimuth for source is obtained by interpolating the recorded data. The azimuth for only a nearby source can be estimated because LD is undetectable at normal conversational sound level when the source is located relatively far from the sensors. In LD estimation, *a priori* knowledge of the environment is necessary in order to determine the azimuth for only nearby sources.

The third is the phase differences (PDs) to which TD is transformed in the frequency domain [12,13]. As PDs are greatly influenced by reverberation similar to TD, an arbitrary azimuth for source is estimated by interpolating the phase difference spectral patterns recorded for various source azimuths in the same manner as LD estimation. The prepared database depends on the surrounding environment in PDs estimation.

In the present paper, a new algorithm is proposed that provides precise and real-time localization of an acoustic

*e-mail: shimo@ee.cit.nihon-u.ac.jp

source, even under reverberation, using two sensors. The azimuth on the horizontal plane for a single source, which is located relatively distant from the two sensors, is identified from the general linear relationship on the frequency - phase difference plane, which is extracted from the measured phase difference spectrum after filtering. The phase difference spectrum is introduced as the quasi-stationary cross-spectral phase between the sound-signals detected simultaneously by two sensors.

In Section 2, the principle of the present algorithm is described. The relationship between the propagation path difference and the azimuth for source, as well as the path difference dependency on the distance between source and sensors, are given.

In Section 3, the measurement and computational procedures are presented, including techniques for measuring the phase difference spectrum, filtering, the general slope approximation on the phase difference spectrum, and the identification of the source azimuth.

Section 4 presents a number of examples regarding acoustic source localization in an anechoic chamber. Two different types of source, white noise and voice, are used for the source localization under the same condition. The azimuths for various source positions are identified. The source localization accuracy is presented. As more complicated examples, the source localizations at the center and beside the wall in the corner of the reverberant room are shown. Both the white noise source, which is located approximately 4.7 m from the sensors, and the open-air noise source through a slightly open door, are localized.

2. METHOD

2.1. Propagation Path Difference and Azimuth for Source

Let us consider the case in which the sound is radiated from a point source. A pair of sensors (Mic1, 2) positioned at a distance D from the source and separated by the interval S is used to detect the sound signals, as shown Fig. 1.

The phase difference $\Delta\phi$ between the sound pressures is expressed as a function of the propagation path difference Δd between $\overline{AE}$ and $\overline{BE}$ at an arbitrary frequency

$$\begin{aligned}\Delta\phi &= \frac{\Delta d}{\lambda} \times 360 \\ &= \frac{\Delta d}{c} f \times 360 \quad (\text{deg})\end{aligned} \tag{1}$$

where λ is the wave length, c is the sound velocity (constant), and f is the frequency. Both sides of Eq. (1) are then differentiated by f and the slope α of the phase difference spectrum is introduced on the frequency - phase difference plane.

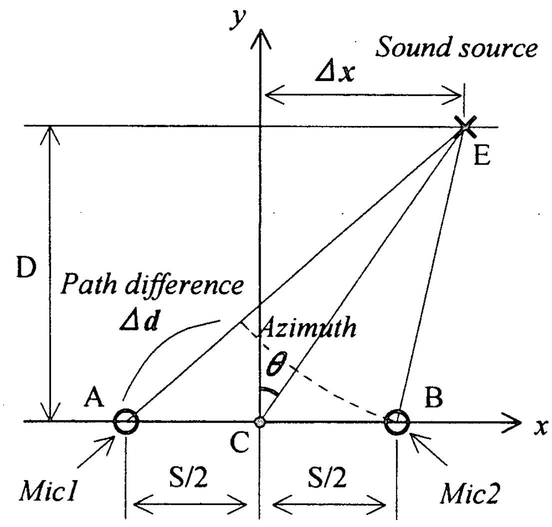

Fig. 1 Geometry of sound source and a pair of sensors (a plane view).

$$\alpha = \frac{d(\Delta\phi)}{df} = \frac{\Delta d}{c} \times 360 \quad (\text{deg/Hz}) \tag{2}$$

The slope α of the phase difference spectrum depends only on the path difference when the sound velocity is constant. Equations (1) and (2) imply that the phase difference spectrum of sound pressure radiated from a single source is theoretically a straight line.

Next, let us examine the relationship between the propagation path difference and the azimuth for source on the horizontal plane. The path difference is calculated using the principles of plane geometry as follows (see Fig. 1).

$$\begin{aligned}\overline{AE} &= \sqrt{D^2 + (S/2 + \Delta x)^2} \\ \overline{BE} &= \sqrt{D^2 + (S/2 - \Delta x)^2} \\ \Delta d &= \overline{AE} - \overline{BE}\end{aligned} \tag{3}$$

$$= \sqrt{D^2 + (S/2 + \Delta x)^2} - \sqrt{D^2 + (S/2 - \Delta x)^2} \tag{4}$$

The azimuth for source θ is expressed as

$$\theta = \frac{360}{2\pi} \arctan\left(\frac{\Delta x}{D}\right) \quad (\text{deg}) \tag{5}$$

Using Eqs. (1), (4) and (5), a number of theoretical examples of the phase difference spectrum are shown in Fig. 2. The phase difference spectrum may be a discontinuous function of frequency. The discontinuities will be jumps of 360°. As the frequency decreases, the value of the phase difference approaches zero. The phase difference spectrum passes through the origin. The absolute value of the spectrum slope is found to decrease for smaller azimuth.

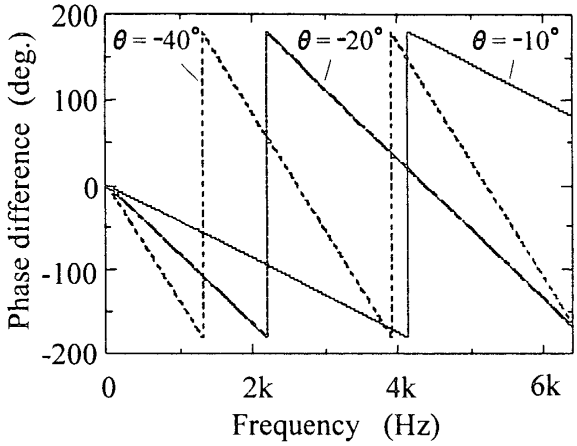

Fig. 2 Calculated phase difference spectra of sound pressure.

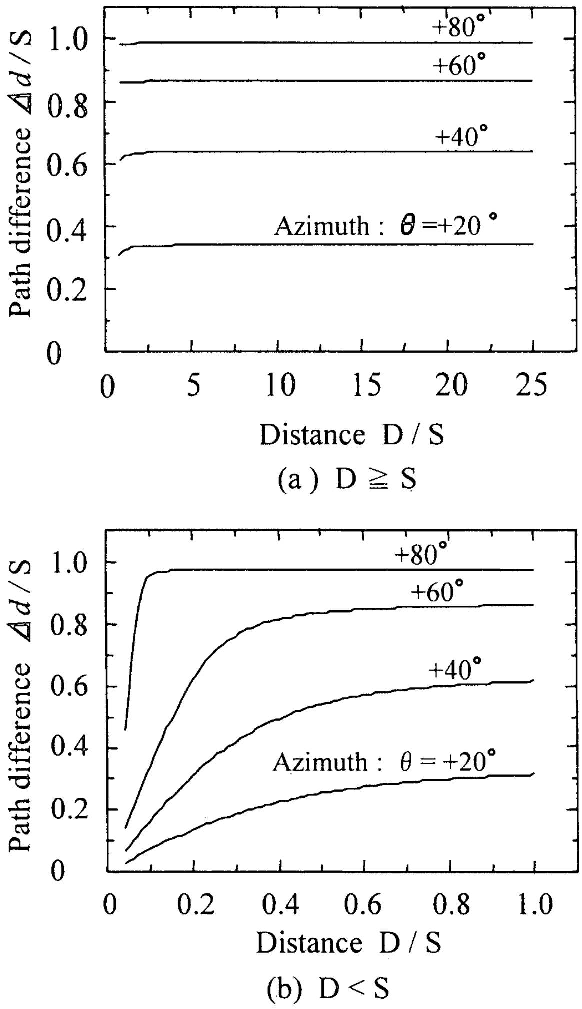

Fig. 3 Path difference dependency on the distance between source and sensors (normalized with the sensor interval S).

2.2. Path Difference Dependency on Distance between Source and Sensors

The distance between source and sensors is assumed as *a priori* knowledge in Eqs. (4) and (5), see D in Fig. 1. This condition is unrealistic in the localization of sound. The propagation path difference dependency on the distance between source and sensors is shown for a number of source azimuths in Fig. 3. The path difference does not change greatly with distance under the condition in which the distance from the source to the sensors is greater than the sensor interval S, $D \gg S$, as shown in Fig. 3(a). The path difference value at $D/S = 2.5$ is approximately 2% less than that at $D/S = 20$ for the source azimuth $+20°$. On the other hand, the path difference changes according to not only the distance but also the azimuth for source when the source is located near the sensors, $D < S$, as shown in Fig. 3(b). One-to-one correspondence between the path difference and the azimuth for source can be found only under the condition $D \gg S$. An arbitrary distance from the sensors that is greater than the sensor interval S should be substituted for D in Eqs. (4) and (5). The estimation of slope α in Eq. (2) is equivalent to searching the azimuth for source in space under $D \gg S$.

3. SOURCE LOCALIZATION PROCEDURE

A kind of inverse problem may be solved in order to estimate the azimuth for source using the measured sound pressures. In order to localize the acoustic source in a real environment, a number of procedures are required for overcoming the difficulties associated with measuring, for example, the repeatability and adaptability to various environments. In the present paper, the relationship between the phase differences in the frequency domain is utilized as the acoustical cue of the sound pressure. The sound source localization procedure is outlined in Fig. 4. The procedure is composed of the following four operations.

3.1. Measuring Phase Difference Spectrum

The time-dependent sound signal waveforms detected simultaneously using each of the omni-directional microphones, are multiplied by a Hanning window and are transformed from the time domain to the frequency domain via a DFT algorithm. The corresponding output pairs in frequency domain are multiplied to form the cross spectrum. The phase difference spectrum obtained as the cross-spectral phase is overlapped and averaged over time.

3.2. Filtering Phase Difference Spectrum

The phase difference spectrum, which is measured in the reverberant room for the case in which the source is located far from the microphones, tends to be distributed at random on the frequency - phase difference plane due to the influence of the reverberation. All of the phase difference spectrum may not always contribute to the localization of the target source. Therefore, the phase difference spectrum is filtered under the rule in which the "cluster" is selected. Here, the "cluster" indicates the group

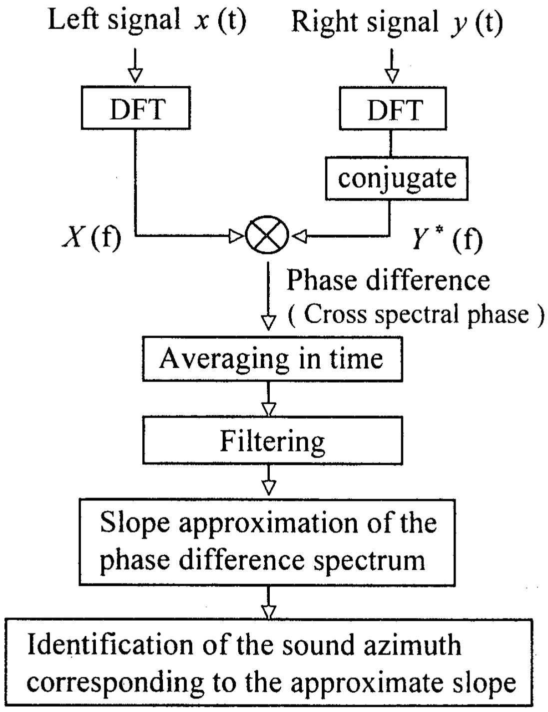

Fig. 4 Proposed algorithm for source localization.

of the phase difference data in which values are similar in frequency. The filtering algorithm is as follows:

(i) On the frequency-phase difference plane, the measured frequency span is divided into L sections, where the phase difference span is divided into M sections, see Fig. 5. The entire plane is then divided into $L \times M$ sections.

(ii) The number of the phase difference data contained in each section is calculated.

(iii) The maximum number of data contained in the section, N_{max} is determined.

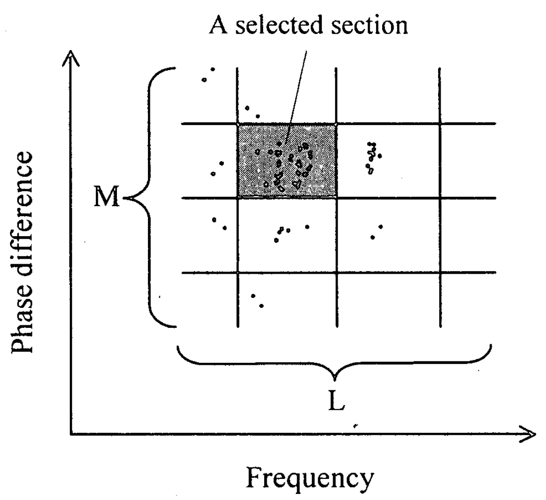

Fig. 5 Filtering the sections for evaluation on the frequency - phase difference plane based on the number of the data contained in each section.

(iv) Data in sections which contain less than $N_{\mathrm{max}} * C$ data are not used for evaluation, where C is the filtering constant ($0 \leqq C \leqq 1$).

As the phase difference spectrum is a one-valued function of frequency, the filtering procedure determines the appropriate frequencies for evaluation.

These constant values, C, L and M are adjustable, allowing adaptability to various acoustic environments in the present algorithm. That these constant values may be set in advance for typical known acoustic sources in certain environments is desirable. The source azimuth identification is not so sensitive to these constant values, as will be described later.

3.3. Slope Approximation

The spectral slope α in Eq. (2) using the filtered phase difference spectrum is approximated as follows.

Let us assume a straight line inclined α which passes through the origin on the frequency - phase difference plane. The theoretical phase difference value can be calculated on the assumed straight line at arbitrary frequency. The optimum value of α is obtained such that the norm between the filtered phase difference spectrum and the calculated spectrum is minimized by scanning its slope.

As a definite form, the norm ε defined in Eq. (6) is numerically minimized over the frequency range from f_{L} to f_{H}. Then, the optimal slope α is obtained when the norm ε is minimized

$$\varepsilon = \sum_{i=1}^{N} (\Delta\phi_i - \alpha f_i)^2 \quad (\mathrm{deg}^2) \tag{6}$$

where f_i is the frequency, $\Delta\phi_i$ is the filtered phase difference value at f_i, and N is total number of frequencies selected for evaluation in Section 3.2. This procedure extracts a general linear relationship from the filtered phase difference spectrum on the frequency - phase difference plane.

3.4. Calculation of Source Azimuth

Equation (2) can be expressed in the following form.

$$\Delta d = \frac{\alpha c}{360} \quad (\mathrm{m}) \tag{7}$$

If the optimal slope value is substituted for α in Eq. (7), the path difference Δd corresponding to the azimuth for source is obtained. Then, Δx is numerically searched, where the error in Eq. (8) is minimized.

$$\begin{aligned} error = \Big| \Delta d - \Big(& \sqrt{D^2 + (S/2 + \Delta x)^2} \\ & - \sqrt{D^2 + (S/2 - \Delta x)^2} \Big) \Big| \end{aligned} \tag{8}$$

Equation (8) is obtained from Eq. (4). Finally, the azimuth for source is calculated in Eq. (5).

Finding the optimal slope α in Eq. (6) is equivalent to searching the azimuth for source not only in space but also in frequency.

4. APPLICATION

In order to confirm the experimental accuracy for the source localization, the sound was radiated through a speaker driver, which was connected to a copper tube (length: 12 cm, inner diameter: 8 mm) via a tapered cast-nylon tube. The acoustic source was localized for two sound signals — white noise and voice (BBC News), which were recorded and reproduced using a tape recorder. Two microphones (Type 4190, B&K) were fixed in the same direction at a 20-cm interval using a tripod.

The frame period was set to 500 ms in the DFT procedure. The phase difference spectrum was measured as the cross-spectral phase, which was overlapped 75%, and was the average of ten measurements conducted using a multi-analyzer system (Pulse 3560C, B&K). The sound signal was treated as quasi-stationary by time averaging over the total measurement period for approximately 1.6 s. Averaging fewer measurements deteriorates the repeatability of the measurement. The cross-spectral phase was measured over the frequency range from 0 (f_L) to 6.4 kHz (f_H), which nearly contain the main formant frequencies of the voice sound signal.

4.1. Source Localization in an Anechoic Chamber

The speaker driver was placed 48 cm (D in Fig. 1) from the two microphones in a 1.1-m^3 anechoic chamber having a metal base plate. The flat metal base plate covered with glass wool functions as a kind of sound reflector in the anechoic chamber. Figure 6 shows the phase difference spectra measured for several white noise source azimuths. As the source azimuth increases, the general slope of the phase difference spectrum increases. Each spectrum shows a ripple. The results of similar experiments conducted in a larger anechoic room having no sound reflector revealed that interference between direct sound and reflected sound may be the primary cause of the ripple because the ripple was only barely noticeable in the spectrum obtained in the larger anechoic room.

The sound pressure amplitude spectra for the white noise and voice are shown in Fig. 7. The amplitude of each spectrum was obtained by time averaging ten measurements performed using Mic1, shown in Fig. 1. Corresponding to Fig. 7, Fig. 8 compares the white noise and voice sound signals with respect to the measured phase difference spectrum and the identified spectrum. Although the amplitude spectrum for the white noise sound signal was found to differ remarkably from that of the voice sound signal, as shown in Fig. 7, the phase difference spectra differed only slightly, as shown in Figs. 8(a) and (b). The

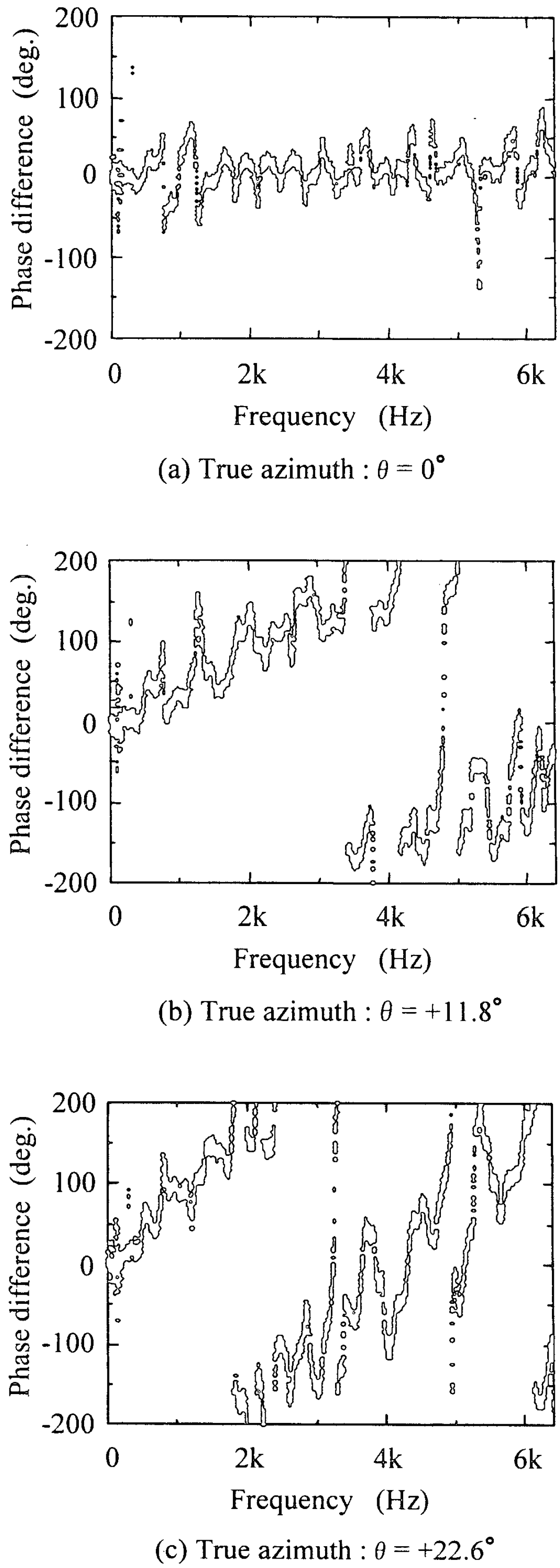

Fig. 6 Measured phase difference spectra in an anechoic chamber having metal base plate.

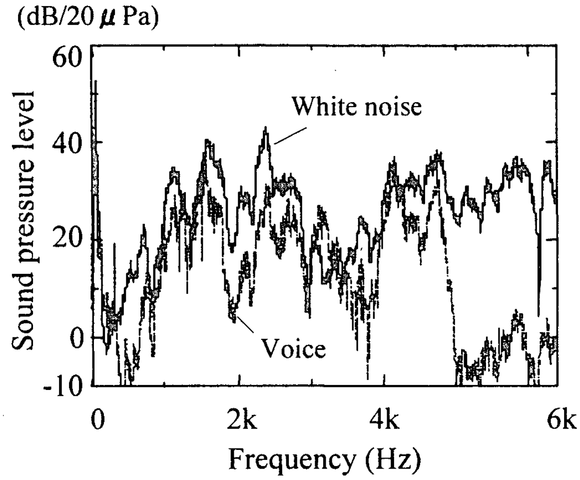

Fig. 7 Sound pressure amplitude spectra measured using Mic1 in an anechoic chamber after time averaging ten measurements.

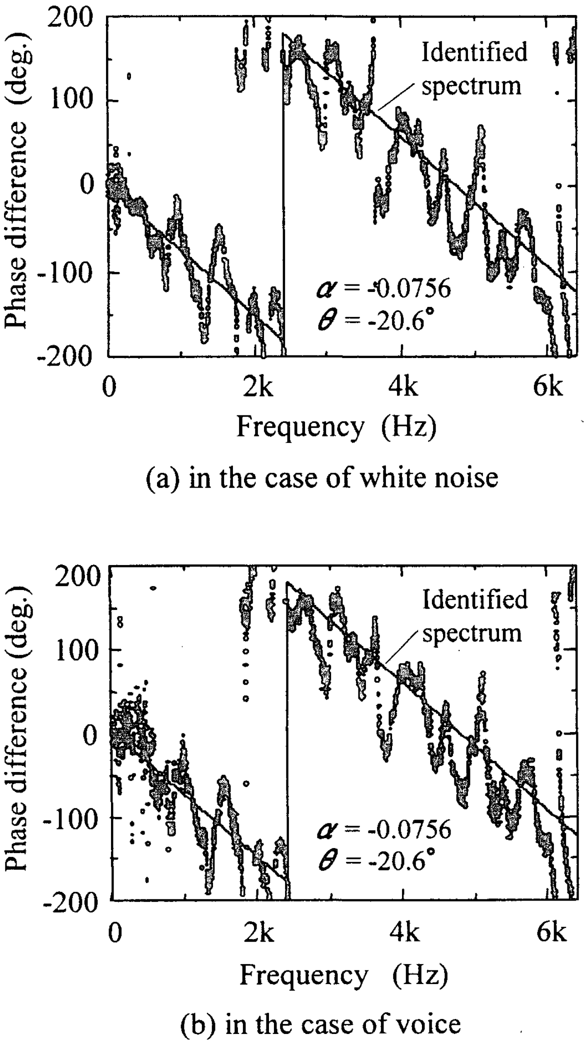

Fig. 8 Comparison of the white noise and voice sound signals with respect to measured phase difference spectrum and the identified spectrum (in an anechoic chamber, True azimuth: $\theta = -22.6°$, $C = 0$).

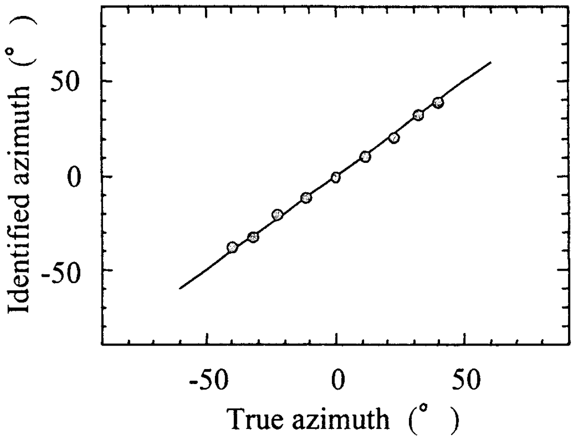

Fig. 9 Comparison of true azimuth with identified for various source locations.

phase difference spectrum was not affected by the type of sound signal, except at either frequencies lower than 1 kHz or at approximately 5 kHz when the sound pressure level is too low to be detected precisely, especially in the case of the voice sound signal. This indicates that the phase difference can be precisely detected even in the case of very low-level sound. The identified spectrum passes through the center along the distribution shown in Figs. 8(a) and (b). In both cases, the optimal spectral slope was identified as $-0.0756°$/Hz and the corresponding source azimuth was $-20.6°$, with an error of approximately $+2°$ (true azimuth was $-22.6°$). The filtering did not contribute to identification of the source azimuth in the above experiments.

The comparison of true azimuth with identified for various source locations is shown in Fig. 9. The azimuths for source were identified within an error of $\pm 2°$ over the azimuth range, from approximately $-40°$ to $+40°$.

4.2. Source Localization at the Center in the Reverberant Room

The phase difference spectra were measured at the center of the reverberant room (approximately 11.2 m in length, 7.2 m in width and 2.7 m in height). The room has good echo characteristics, because the exposed concrete walls face each other. The white noise source was located 3 m from the microphones ($D = 3$ m in Fig. 1). Figure 10 shows the measured phase difference spectra for different source locations. Each phase difference spectrum is widely distributed from $-200°$ to $+200°$. Although the measured phase difference spectrum has less continuity as a function of frequency, a line representing the distribution of the data (dots) is observed on the frequency - phase difference plane. The general slope of the phase difference spectrum changes with the azimuth for source. Comparisons of the filtered phase difference spectra with the identified spectra are shown in Fig. 11. The filtering constant was set to 0.45,

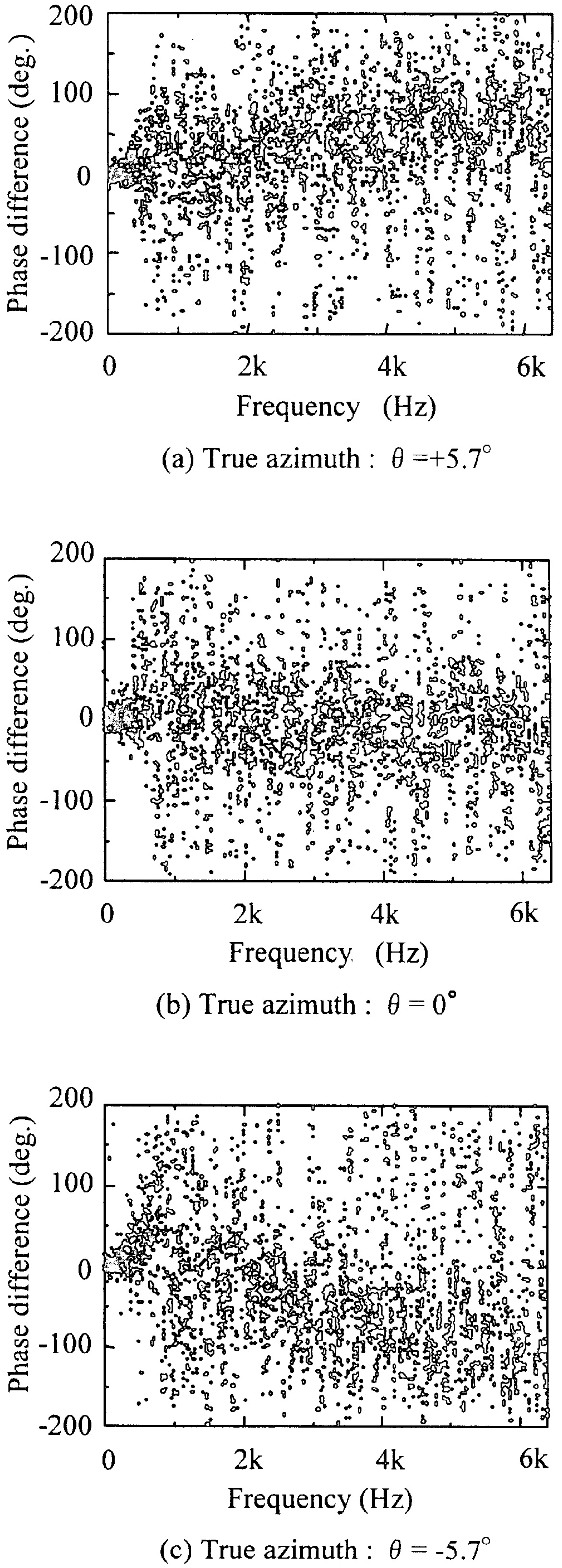

Fig. 10 Phase difference spectra measured at the center of the reverberant room (White noice, $D=3$ m).

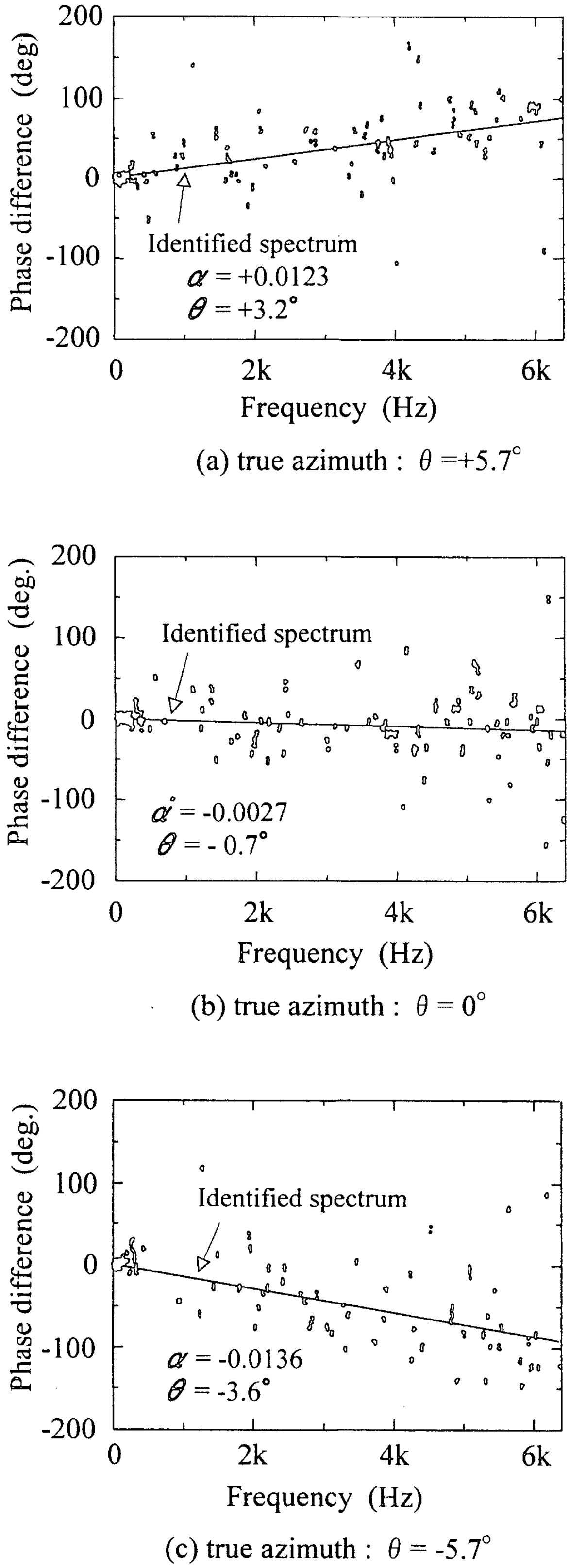

Fig. 11 Filtered phase difference spectra and the identified spectra (at the center of the reverberant room, White noise, $D=3$ m, $C=0.45$).

where the frequency span was divided into 200 sections and the phase difference span was divided into 50 sections ($C = 0.45$, $L = 200$, $M = 50$ in Section 3.2). The optimal spectral slopes were identified as (a) $+0.0123°$/Hz, (b) $-0.0027°$/Hz, and (c) $-0.0136°$/Hz, respectively. The corresponding sound azimuths were (a) $+3.2°$, (b) $-0.7°$, and (c) $-3.6°$, with an error of approximately $\pm 3°$.

4.3. Source Localization Near the Wall in the Reverberant Room

For more complicated applications, the azimuths for various source types were identified. Figure 12 shows the reverberant room layout. Two microphones were placed approximately 45 cm from the exposed concrete wall. The room had a door and a speaker driver was placed at the corner of square strut on the right-hand side. An air-conditioner diffuser was located on the left-hand side of the ceiling.

The white noise through the speaker driver located approximately 4.7 m from the microphones was localized for the case of no air-conditioning. Figure 13 shows the measured phase difference spectrum (a) before filtering and (b) the comparison of the measured spectrum with that identified after filtering ($C = 0.45$, $L = 200$, $M = 50$). The filtering extracts parts of the cluster as the images on the frequency - phase difference plane. The azimuth for source was precisely identified from the extracted images on the phase difference spectrum.

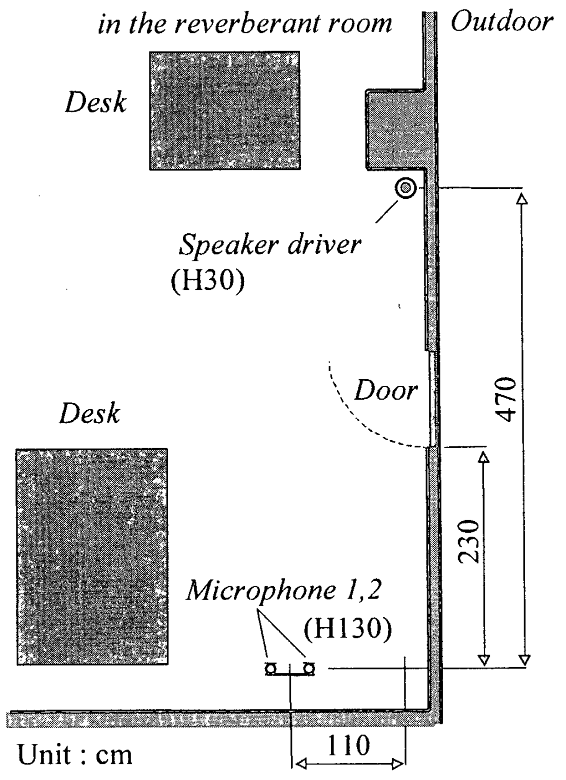

Fig. 12 Reverberant room layout.

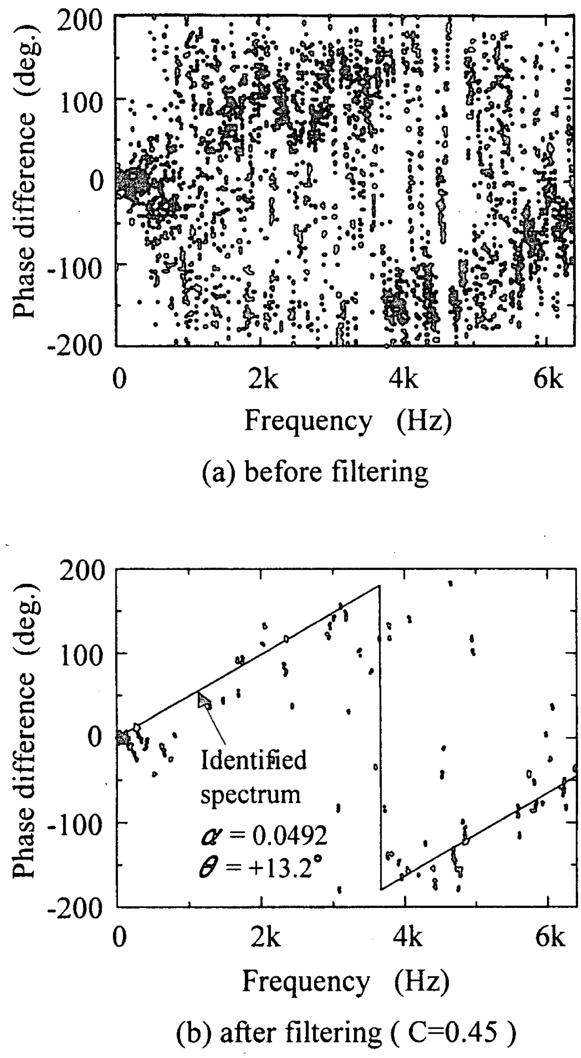

Fig. 13 Localization for white noise source placed beside the wall ($D = 4.7$ m, True azimuth: $\theta = +13°$).

Next, the azimuth for the open-air noise through the slightly open door was identified in the absence of any other noise for the case of no air-conditioning. No particular noise, other than traffic noise far from the room, entered the room. The amplitude spectrum detected by Mic1 and the corresponding phase difference spectrum, are presented in Figs. 14 and 15, respectively. The sound pressure level of open-air noise was observed to decrease gradually for higher frequencies, with the exception of a number of peaks, as shown in Fig. 14. A belt of clusters at frequencies lower than 2 kHz is observed, whereas the phase difference spectrum is distributed almost randomly at frequencies higher than 4 kHz, as shown in Fig. 15. Figure 16 shows the sound azimuth identification dependency on the filtering constant. The identified sound azimuth does not agree with the true azimuth for (a) $C = 0.3$. In contrast, the identified sound azimuth agrees well with the true azimuth for (b) $C = 0.4$ and (c) $C = 0.5$ ($L = 200$, $M = 50$). The filtering procedure is required in order to identify the azimuth for source from the faded images on

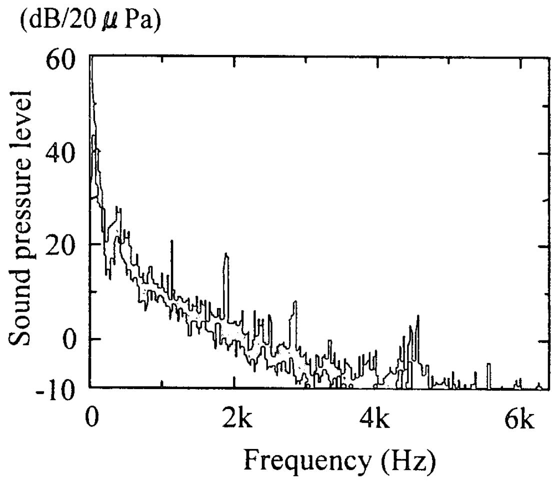

Fig. 14 Measured sound pressure amplitude spectrum of open-air noise through the slightly open door ($D = 2.3$ m).

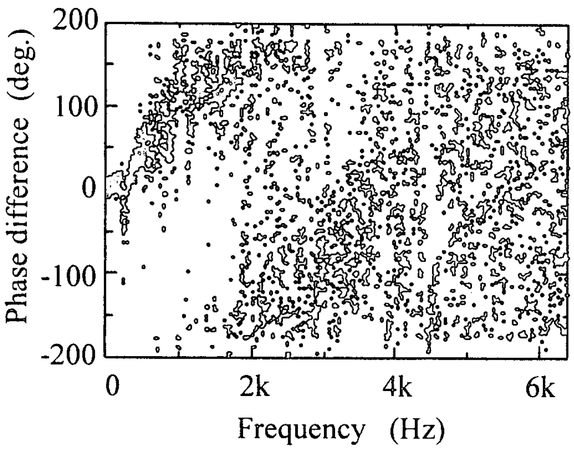

Fig. 15 Measured phase difference spectrum of open-air noise through the slightly open door ($D = 2.3$ m).

the phase difference spectrum. Figure 17 shows the distributions of the norm ε in Eq. (6) on the source azimuth for the filtering constant C ($L = 200$, $M = 50$). Although the norm takes a minimum value at approximately 0° in the cases of $C = 0.1$ and $C = 0.3$, the norm takes a minimum value at true azimuth (20–29°) in the case of $C = 0.4$–0.8. The identified azimuths in which the norm in Eq. (6) is minimized are shown with respect to the filtering constant C and with respect to the number of divisions L and M in Figs. 18(a), (b) and (c), respectively. The identified azimuths agree well with the true azimuths for filtering constants larger than 0.38, for a number of frequency divisions greater than 100, and for almost all numbers of phase difference divisions ranging from 10 to 70, as shown in Figs. 18(a), (b) and (c), respectively. The source azimuth identification was not exceedingly sensitive for the constants, C, L and M, so that changing these constants individually was not necessary in the above experiments. As these constants occasionally affect the

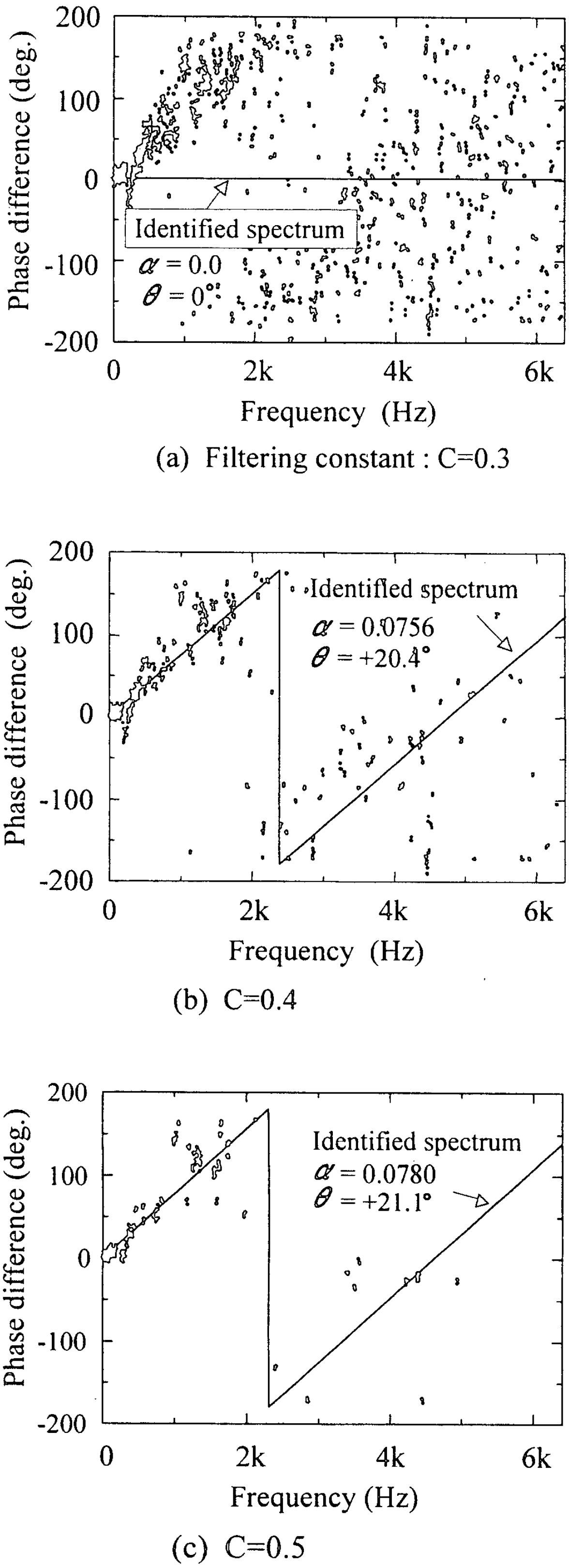

Fig. 16 Source azimuth identification dependency on filtering constant C (open-air noise through the slightly open door, $D = 2.3$ m, true azimuth: 20°–29°).

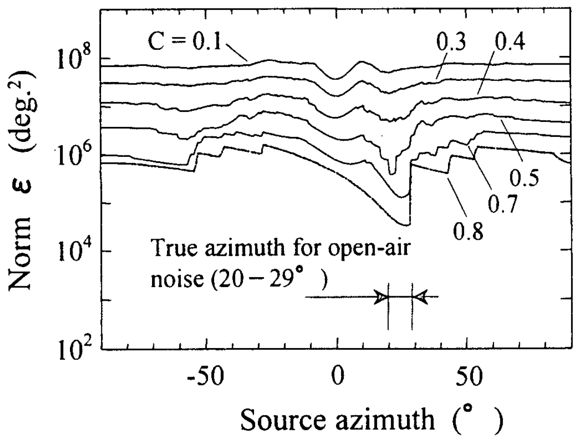

Fig. 17 Distribution of the norm ε (in Eq. (6)) on the source azimuth for the filtering constant (open-air noise through the slightly open door, $D = 2.3$ m, $L = 200$, $M = 50$).

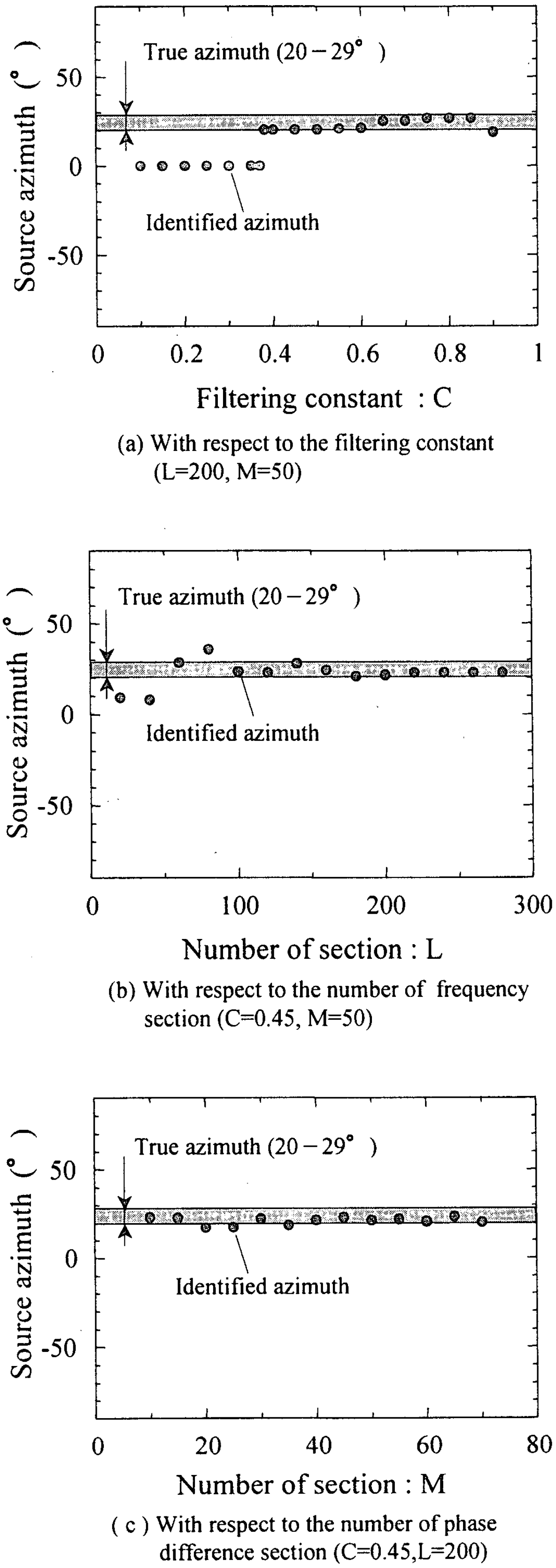

Fig. 18 Identified azimuth with respect to the filtering constant C and the number of division L and M (open-air noise through the slightly open door, $D = 2.3$ m).

accuracy of the sound azimuth identification, careful attention should be given to the selection of suitable constants according to the measured spectrum. Otherwise, an additional procedure, for example, filtering with respect to the sound pressure level, should be introduced to the present algorithm.

Finally, three types of spectral patterns on the frequency - phase difference plane are shown in Fig. 19. Each spectral pattern is generated by marking the selected section black after filtering. The marked sections are distributed in differently corresponding to the various acoustic conditions. If the spectral patterns are recorded as a database corresponding to typical acoustic scenes in advance, the surrounding acoustic scene may be estimated by matching a specific spectral pattern.

5. CONCLUSION

The azimuth on the horizontal plane for a single acoustic source, which was located relatively far from two sensors, was identified from a general linear relationship on the frequency - phase difference plane, which was extracted from the measured phase difference spectrum after filtering. The phase difference spectrum was introduced as the quasi-stationary cross-spectral phase between the sound-signals detected simultaneously by two sensors. The results of the present study are as follows. First, the phase difference spectrum was hardly affected by the sound pressure level, but was affected by the azimuth for source. Second, although the measured phase difference spectrum had less continuity as a function of frequency, a linear distribution of the images obtained from the data was observed on the phase difference spectrum. Finally, using the images on the phase difference spectrum, the sound azimuths for various sources, located at a distance from the sensors that is greater than the sensor interval and radiating any kind of broadband sound on a separated time schedule,

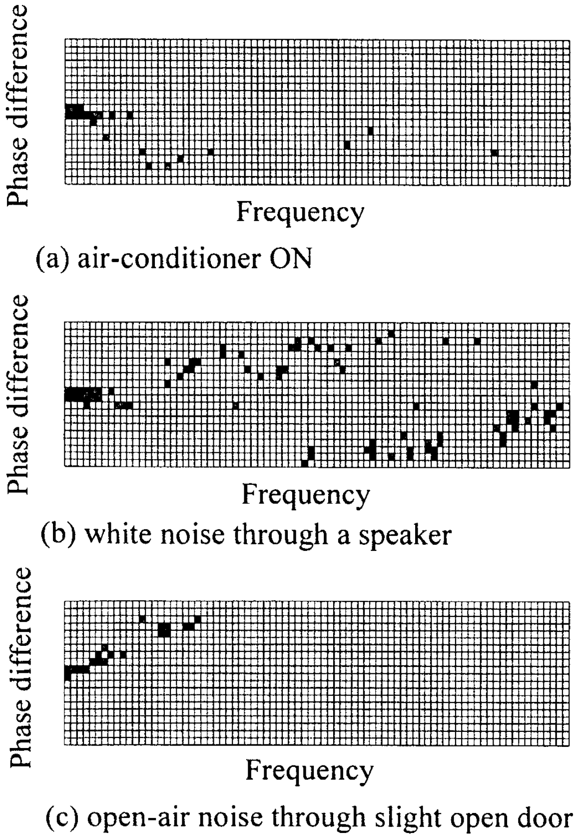

Fig. 19 Filtered phase difference spectral patterns for various acoustic conditions in the reverberant room ($C = 0.45$, $L = 80$, $M = 20$).

could be precisely identified even in a reverberant room. Careful attention should be given to the selection of the filtering constant C and the number of divisions L and M according to the measured spectrum. In order to improve the adaptability to various environments, the optimization technique, which allows the constants C, L and M to be optimized may be introduced to the present algorithm.

An interesting potential application of the present algorithm to the binaural model is the use of a dummy head for furthering our understanding of the human auditory system. Source localization using more than two sensors, which would allow two- or three-dimensional localization, as well as localization of multiple sources, is also possible using the proposed algorithm. The real-time display on the phase difference spectrum using multiple sensors would enable an acoustic-camera, a sound version of the TV camera. In addition, the application of the proposed algorithm to various physical phenomena having a wave nature may provide interesting and exciting insights.

ACKNOWLEDGEMENT

This study was supported by a Grant for High Technology Research Projects, from the Ministry of Education, Culture, Sports, Science and Technology of Japan.

REFERENCES

[1] L. Rayleigh, "On our perception of sound direction," *Philos. Mag.*, **13**, 214–232 (1907).
[2] S. S. Stevens and E. B. Newman, "The localization of actual sources of sound," *J. Psychol. Am.*, **48**, 297–306 (1936).
[3] R. A. Butler, "The influence of the external and middle ear on auditory discriminations," in *Auditory System*, W. D. Keidel and W. D. Neff, Eds. (Springer-Verlag, NewYork, 1975), Chap. 6, pp. 247–260.
[4] N. I. Durlach and H. S. Colburn, "Binaural phenomena," in *Handbook of Perception*, E. C. Carterette and M. P. Friedman, Eds. (Academic Press, 1978), Chap. 10, pp. 365–466.
[5] F. L. Wightman and D. J. Kistler, "Sound localization," in *Human Psychophysics*, W. A. Yost, A. N. Popper, R. R. Fay, Eds. (Springer-Verlag, NewYork, 1993), Chap. 5, pp. 155–192.
[6] A. S. Bregman, "Auditory scene analysis: Hearing in complex environment," in *Thinking in Sound*, S. McAdams, E. Bigand, Eds. (Clarendon Press, Oxford, 1993), Chap. 2, pp. 10–36.
[7] L. A. Jeffress, "A place theory of sound localization," *J. Comp. Physiol.*, **41**, 35–39 (1947).
[8] B. Champagne, M. Eizenman and S. Pasupathy, "Exact maximum likelihood time delay estimation for short observation intervals," *IEEE Trans. Signal Process.*, **39**, 1245–1257 (1991).
[9] B. G. Ferguson, "Time-delay estimation techniques applied to the acoustic detection of jet aircraft transits," *J. Acoust. Soc. Am.*, **106**, 255–264 (1999).
[10] Y. Haneda, S. Makino, Y. Kaneda and N. Kitawaki, "Common-acoustical-pole and zero modeling of head-related transfer functions," *IEEE Trans. Speech Audio Process.*, **7**, 188–196 (1999).
[11] I. Kinoshita and S. Aoki, "Representation of sound localization transfer function and psychoacoustical evaluation," *J. Acoust. Soc. Jpn. (E)*, **20**, 271–280 (1999).
[12] M. Aoki, M. Okamoto, S. Aoki, H. Matsui, T. Sakurai and Y. Kaneda, "Sound source segregation based on estimating incident angle of each frequency component of input signals acquired by multiple microphones," *Acoust. Sci. & Tech.*, **22**, 149–157 (2001).
[13] H. Okuno and K. Nakadai, "Are a pair of ears sufficient for robot audition?," *J. Acoust. Soc. Jpn. (J)*, **58**, 205–210 (2002).

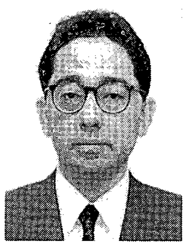

Ryuichi Shimoyama received B.E. and M.E. degrees in Electrical Engineering from Toyama University in 1979, 1981 respectively and received Ph.D. degree in System Science from Okayama University, in 1994. He is a Lecturer in College of Industrial Technology, Nihon University. His current research interests include artificial intelligence on auditory system. He is a member of ASJ, IEICE, IPSJ and JSST.

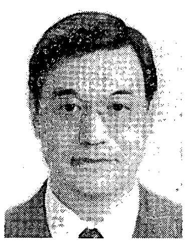

Ken Yamazaki received Dr.Sci. degree from Okayama University, Japan, in 1993. He is currently a Professor at Nihon University in Japan. He investigated in Sothampton University UK as a guest researcher by 1992 since 1989. His research interests are the visualization and numerical simulation of the sound field, the creation of the comfortable sound space, *et al.* He is a member of ASJ, JSST, IEICE, AIJ in Japan and ASA in USA.